

Original Paper

Design and Simulation of an Igniter for Surrounding-Type Underground In-Situ Coal Gasification

Hao Wang^{1,2,3}, Ke Gao^{1,2,3}, Yumin Wen^{1,2,3}, Xiaoshu Lv^{1,2,4}, Xiaobo Xie^{1,2,3}, Xu Li^{1,2,3}, Fan Yang⁵, Yan
Zhao^{1,2,3*}

¹ College of Construction Engineering, Jilin University, Changchun 130061, China

² Key Laboratory of Drilling and Exploitation Technology in Complex Conditions, Ministry of Natural Resources, Jilin University, Changchun 130061, China

³ Engineering Research Center of Geothermal Resources Development Technology and equipment, Ministry Education, Jilin University, Changchun 130061, China

⁴ Department of Electrical Engineering and Energy Technology, University of Vaasa, Vaasa FIN-65101, Finland

⁵ Engineering Geology Research and Development Center, Beijing Institute of Ecological Geology, Beijing 100039, China

* Corresponding Author: Zhao Yan, E-mail: zhaoyan1983@jlu.edu.cn

Received: October 20, 2024 Accepted: November 16, 2024 Online Published: November 19, 2024

doi:10.22158/asir.v8n4p120 URL: <http://doi.org/10.22158/asir.v8n4p120>

Abstract

To optimize the gas passage of underground coal igniters and enhance the performance and efficiency of ignition heaters, meeting the demands of actual underground operations, this paper designs a set of annular ignition heaters. By simulating the internal gas flow within the igniter, the pressure distribution and velocity characteristics inside the igniter are analyzed. Utilizing combustion flow field simulation technology, a comparison is made between the heating and ignition effects of annular igniters and central igniters in coal heating. The performance of the deflecting tube under different eccentric angles is simulated to determine the optimal eccentric angle for achieving the best heating effect. The results indicate that annular igniters for underground in-situ coal gasification have significant advantages over traditional igniters in terms of wellbore heating and flame penetration, with the optimal eccentric angle of the igniter being 10°.

Keywords

underground coal gasification, combustion flow field, simulation analysis, igniter

1. Introduction

Underground Coal Gasification (UCG) is an innovative coal mining method that involves directly controlled combustion of coal underground, converting it into combustible syngas such as CH₄ and H₂ through advanced engineering techniques and processes (Adjei, Yindi, Mengting, et al., 2023; Stefan, Erika, Andrea, et al., 2021; Mao, 2016). After undergoing multi-stage treatment at the surface, these syngas can be further converted into raw materials and energy required by industries. This technology has opened up a new path for the clean and efficient utilization of coal resources and the production of chemical raw materials (Yang, Duan, Ma, et al., 2020). UCG represents a revolution in traditional coal mining methods, as it eliminates the need for personnel to work underground, effectively preventing casualties and mine disasters, and provides a new utilization pathway for coal resources that are difficult to extract using traditional methods due to complex geological conditions, deep coal seams, and high gas content. At the same time, it effectively avoids the destruction of the underground natural environment and is characterized by high safety, fast production efficiency, and environmental friendliness (Ma, 2014).

Between 1868 and 1888, German scientist Wilhelm Siemens first proposed the theory of underground in-situ mining of coal, while Soviet scientist Dmitri Mendeleev outlined the basic process concept of underground coal gasification, pointing out the basic path to industrialize coal gasification (Siemens, 1868). Before the First World War, American chemist Fritz Bates refined the process flow diagrams for underground coal gasification, and British chemists conducted experiments on underground coal gasification. However, the outbreak of the war halted the development of underground coal gasification technology. In 1932, the Soviet Union resumed experiments to address energy issues, and the world's first underground coal gasification station using a well-type structure was established in the Donbass mining area. Although experiments were temporarily halted during the Second World War, they resumed in the late 1950s. By the 1960s, the Soviet Union had been increasing its industrially-scaled UCG installations, and the technology for underground coal gasification was basically mature and put into industrial production. Due to the abundance of oil and gas resources within the Soviet Union, there was little interest in underground coal gasification technology (Ranade, Mahajani, & Samdani, 2019). The next country to pick up the baton for underground coal gasification was the United States (Hill & Thorsness, 1982). From the 1970s to 1980s, the United States conducted numerous UCG experiments in Wyoming, Centralia, and the Rocky Mountains, which propelled American UCG technology to the forefront of the world. In the late 1980s, due to significant international oil price increases caused by political unrest, there was a global surge in the search for alternative energy sources. Coalbed methane produced through underground coal gasification technology stood out among many energy sources. Many countries, such as the United Kingdom, France, and Spain, also began experimenting with and producing UCG (Chandelle, Jacquemin, L' olle, et al., 1993). In the 1980s, China comprehensively developed and promoted the research and development of underground coal gasification technology, proposing a gasification method suitable for abandoned mines, characterized by "long channels, large

cross-sections, and two stages." Over time, both Chinese and foreign scientists have continuously optimized UCG processes and innovated a series of equipment. With technological updates, people have placed higher demands on the precision and intelligence of underground coal gasification production. How to combine innovative achievements from other fields in the 21st century to improve the precision and intelligence of UCG has become one of the issues in the field of underground coal gasification research.

In the early 20th century, the ignition system began to gain attention as a crucial piece of equipment in the underground coal gasification process. During the initial stages of development of underground coal gasification technology, the design of the ignition system was relatively simple, primarily relying on traditional combustion methods for ignition and heating. With continuous advancements in technology, the performance and efficiency of ignition heaters gradually improved. To better heat the wellbore and ignite the coal during underground coal gasification, this paper presents the design of a circumferential ignition heater. The significance of this design lies in transforming the traditional structure of the ignition device, where fuel gas is supplied centrally and oxygen is supplied around it, into a configuration where oxygen flows through the center and fuel gas is supplied around the perimeter. This paper simulates the gas flow within the ignition heater, analyzes the pressure and velocity within the ignition heater, and through combustion flow field simulations, compares the differences in coal heating and ignition effects between the circumferential ignition heater and the central ignition heater. Additionally, it simulates the appropriate eccentric angle of the diverter tube to achieve the best heating effect.

2. Combustion Head Design

The combustion head structure is a precisely designed component primarily comprising several key parts: the connection port, mixing chamber, flow diversion chamber, and flow guiding chamber, as illustrated in Figure 1. The connection port serves as the interface with the external fuel and air supply system, ensuring smooth entry of fuel and air while maintaining structural sealing. The mixing chamber is responsible for the initial mixing of fuel and air, preparing for the subsequent combustion process. The flow diversion chamber further distributes and guides the mixed fuel-air mixture to the combustion area, ensuring uniform distribution within the combustion chamber. Lastly, the flow guiding chamber, as a crucial area for directing the mixture into the combustion area, matches the shape and size of the combustion chamber, enabling smooth entry and stable combustion of the mixture. Two pipes penetrate through the mixing chamber, flow diversion chamber, and flow guiding chamber, housing the electric igniter and temperature sensor. These components work in coordination to constitute an efficient and stable combustion system for the combustion head. The fuel selected for this simulation is acetylene.

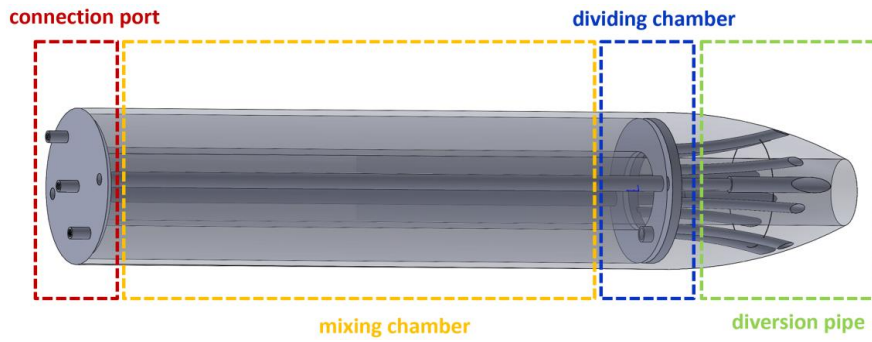


Figure 1. Structural Diagram of the Circumferential Ignition Device Model

3. Simulation of the Flow Field inside the Combustion Head

The internal flow channels of the combustion head are extracted for simulation. After mixing in the fuel gas mixing chamber, the fuel gas and oxygen enter the flow guiding tube through the flow diversion chamber and are ignited by the electric igniter outside the ignition device. By applying a pressure of 10,000 Pa at the connection port to simulate the introduction of oxygen and acetylene into the inlet, a simulation of the flow field inside the combustion head is conducted. The resulting pressure contour inside the combustion head is shown in Figure 2, and the velocity contour inside the combustion head is shown in Figure 3.

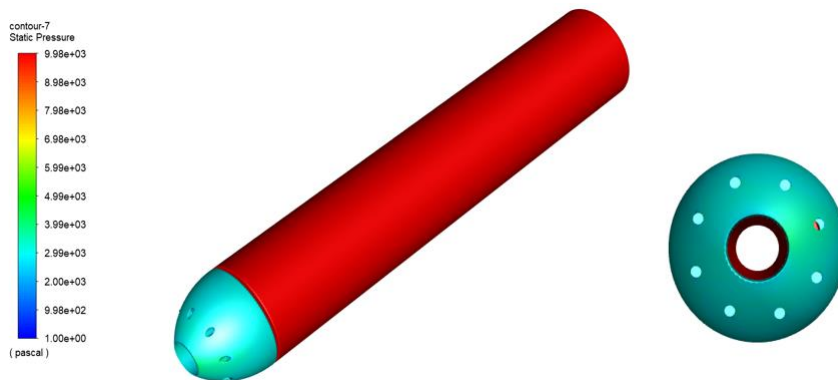


Figure 2. Pressure Contour inside the Combustion Head

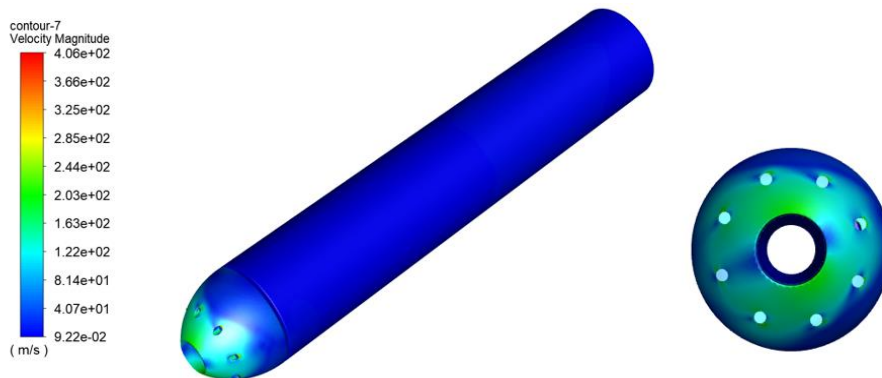


Figure 3. Velocity Contour inside the Combustion Head

Based on the pressure contour analysis, due to the design of the flow diversion chamber, oxygen and acetylene accumulate in the fuel gas mixing chamber, resulting in a gas pressure of up to approximately 10,000 Pa in this area, significantly higher than the 3,000 Pa pressure in the fuel gas diversion chamber. After oxygen and acetylene are uniformly mixed in the fuel gas mixing chamber, due to the significant pressure difference between the two chambers, the mixed gas of acetylene and oxygen rapidly rushes into the flow diversion chamber and is ejected at high speed through the flow guiding tube. This flow characteristic is intuitively reflected in the velocity contour: the flow velocity inside the flow guiding tube is the fastest, followed by the fuel gas diversion chamber, and the fuel gas mixing chamber has the slowest flow velocity. The maximum flow velocity of the mixed gas inside the igniter can reach 400 m/s, far exceeding the flashback velocity of acetylene (approximately 6 m/s). Therefore, the ejection velocity of the fuel gas flow guiding tube is sufficient to ensure that acetylene does not cause an air explosion due to flashback, providing a strong guarantee for the safe operation of the system.

4. Establishment of the Combustion Model

4.1 Geometric Model

The combustion chamber is simplified as a two-dimensional pipeline with dimensions of 1.5m by 0.16m. During the simulation, the igniter has already ignited the mixed gas in the fuel gas mixing chamber. The main oxygen pipeline and fuel gas pipeline continuously inject oxygen and fuel gas into the pipeline to form a stable flame. The circumferential igniter supplies oxygen at the center and fuel gas on both sides, while the central igniter supplies fuel gas at the center and oxygen on both sides, as specifically shown in Figure 4. Oxygen and fuel gas are continuously supplied through the continuous pipes at the ends. The sides of the pipeline are simplified as wellbore walls.

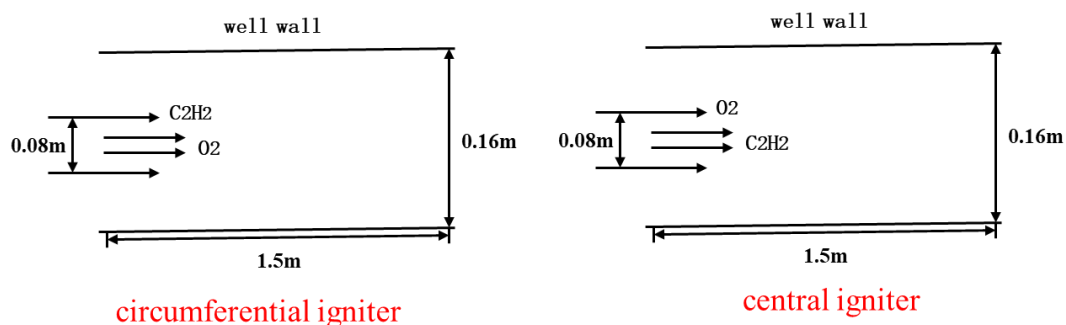


Figure 4. Schematic Diagram of the Geometric Model

4.2 Boundary Conditions

In this paper, the FLUENT software under the ANSYS platform is used to establish the underground combustion chamber model. The underground combustion chamber is simplified as a cylinder with a diameter of 160mm, and the igniter's main oxygen pipeline is arranged concentrically with the combustion chamber. The end face of the igniter's main oxygen pipeline and the fuel gas holes in the

fuel gas mixing chamber serve as the inlets for oxygen and acetylene in the combustion flow field. The inlet boundary is set as a mass flow inlet, and the outlet boundary is set as a pressure outlet. The coal seam near a depth of 1000m underground is selected as the research object, with a formation temperature of 400K and a rock pressure of 10MPa. The specific boundary conditions and operating conditions are listed in Table 1.

Table 1. Boundary Conditions and Operating Conditions

Parameter	Value
Gas inlet temperature (K)	400
Acetylene inlet mass flow rate (kg/s)	0.001
Oxygen inlet mass flow rate (kg/s)	0.001
Wall temperature (K)	400
Formation pressure (MPa)	10
Oxygen concentration	0.5

4.3 Computational Model

The simulated working condition in this paper involves the multicomponent combustion of acetylene and oxygen under various conditions within a combustion chamber. The combustion of acetylene and oxygen in a downhole combustion chamber encompasses complex physical and chemical phenomena. After numerous simulation experiments, the acetylene-oxygen kinetic mechanism was selected as the combustion model. The simulation employs the standard k- ϵ turbulence model to calculate gaseous turbulent transport, and selects the SIMPLEC (Semi-Implicit Method for Pressure-Linked Equations Consistent) pressure-based segregated algorithm. For the simulated heat transfer process, the P1 radiation model, which is suitable for combustion models with large optical depths, is chosen. The gradient term adopts the node-based Green-Gauss format. The pressure term uses a second-order interpolation format. The remaining terms employ a second-order upwind format for higher accuracy. In terms of convergence residuals, the residuals for the continuity equation and momentum equation are set to be less than 10^{-3} ; the residual requirement for the energy equation is less than 10^{-6} .

5. Simulation Results and Their Impacts

5.1 Impact of Heating Method on Combustion Flow Field

With the mass flow rate q of acetylene and oxygen, as well as the oxygen concentration n , remaining constant, the type of igniter was adjusted to simulate the downhole combustion flow field under two operating conditions. Specifically, the circumferential igniter supplies oxygen centrally and fuel gas on both sides, while the central igniter supplies fuel gas centrally and oxygen on both sides. Changes in the igniter type affect the length L of the high-temperature zone on the wellbore wall (where the

wellbore heating temperature exceeding 1000K is considered as the effective heating length). Detailed data are presented in the following table (L_e represents the location of the highest wellbore wall temperature, and T_e represents the highest wellbore wall temperature):

Table 2. Data on Effective Heating Length for Central and Circumferential Igniters

	$q_{C_2H_2}$ (g/s)	q_{O_2} (g/s)	L(m)	L_e (m)	T_e (K)
central igniter	1	1	0.697	0.3885	1630
circumferential igniter	1	1	0.894	0.634	1560

Based on the comparative analysis of the data in the table, we can clearly observe the differences in heating performance between the central igniter and the circumferential igniter. Specifically, the effective heating length of the central igniter is reduced by approximately 28% compared to the circumferential igniter, which means that under the same heating conditions, the circumferential igniter can cover and effectively heat a longer wellbore segment. Additionally, in terms of wellbore wall temperature distribution, the location of the highest temperature induced by the central igniter is advanced by 0.2455 meters compared to the circumferential igniter, due to differences in heat transfer paths and speeds. The peak temperature generated by the central igniter on the wellbore wall is 70 ° higher than that of the circumferential igniter, reflecting a more concentrated heat distribution in the central igniter, whereas the heat distribution in the circumferential igniter is more uniform, effectively avoiding excessively high localized temperatures.

The temperature contour maps of the combustion flow fields for the central and circumferential igniters are shown in Figure 5, where Figure 5a depicts the combustion flow field for the central igniter and Figure 5b depicts the combustion flow field for the circumferential igniter. From the information in the figures, it can be seen that compared to the central igniter, the flame of the circumferential igniter is more vertically continuous within the combustion flow channel, while the flame of the central igniter is more concentrated in the first half of the combustion flow channel and extends radially. Although both produce the same maximum temperature, the temperature distribution within the entire combustion flow channel is more uniform for the circumferential igniter, and the flame shape is more elongated. Furthermore, due to the unique configuration of the circumferential igniter—oxygen in the middle and acetylene on both sides—the flame is formed by the convergence of two streams, with a low-temperature zone between the two flames. In contrast, the low-temperature zone for the central igniter is mainly located at the wellbore wall near the gas inlet, which results in its wellbore heating effect being inferior to that of the circumferential igniter.

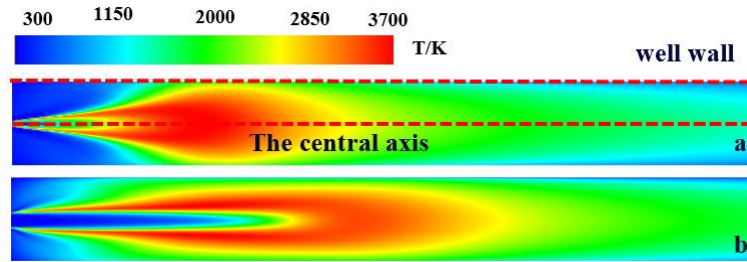


Figure 5. Temperature Contour Maps of Combustion Flow Fields for Central and Circumferential Igniters

The mass fraction distribution maps of acetylene in the combustion flow fields for the central and circumferential igniters are shown in Figure 6, where Figure 6a depicts the combustion flow field for the central igniter and Figure 6b depicts the combustion flow field for the circumferential igniter. According to the information in the figures, in the combustion flow field of the central igniter, acetylene gas is mainly concentrated and extends axially in the middle region of the combustion flow channel. This distribution pattern results in a more pronounced flame shape axially and a relatively weaker flame shape radially. Since acetylene is concentrated in the middle of the combustion flow channel, the high-temperature region of the flame is also concentrated in this area, causing the middle part of the wellbore wall to be more intensely heated. On both sides of the wellbore wall, the lack of acetylene distribution results in weaker heating effects in these areas. In contrast, in the combustion flow field of the circumferential igniter, acetylene gas is divided into two streams and extends radially at a certain eccentric angle. This distribution pattern significantly enhances the flame radially, forming a wider flame surface. Although acetylene is mainly distributed radially, its axial extension exceeds that of the central igniter, due to the unique design of the circumferential igniter that produces a unique flow pattern within the combustion chamber. This flow pattern not only promotes the axial diffusion of acetylene but also enhances the contact area between the flame and the wellbore wall, improving the heating efficiency of the wellbore wall.

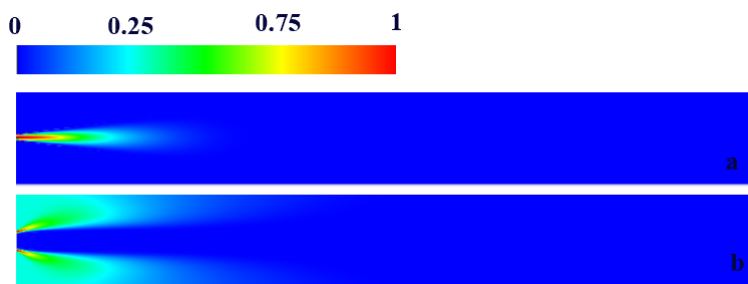


Figure 6. Distribution of Acetylene Mass Fraction in the Combustion Flow Field of Centralized and Surrounding Igniters

The well wall temperature curves for surrounding and centralized heating igniters are shown in Figure 7. The information presented in the figure indicates that, although there may be similarities in the temperature trend along the central axis between surrounding heating and centralized heating, the flame length of surrounding heating is significantly longer. This characteristic allows surrounding heating to more fully utilize heat and enhance the heating effect. Additionally, due to the relatively lower maximum temperature of surrounding heating, it is more conducive to the stable heating and conversion of coal seams. This not only helps improve the conversion rate of coal seams but also reduces harmful emissions generated by high temperatures.

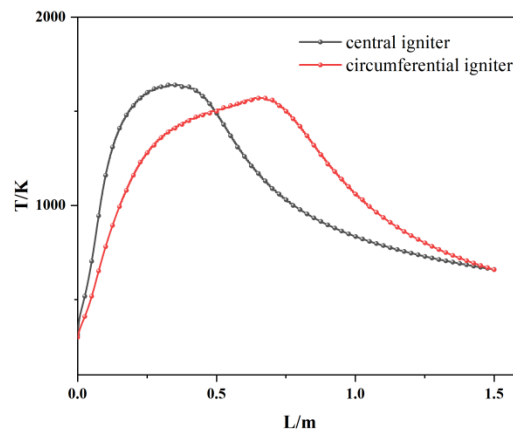


Figure 7. Well Wall Temperature Curve for Surrounding and Central Heating Igniters

Compared to central heating, surrounding heating demonstrates particularly prominent advantages in well wall heating applications. Firstly, in terms of heating length, surrounding heating can cover a wider area, meaning it can more comprehensively heat the well wall and ensure uniform heat distribution. This uniform distribution not only improves heating efficiency but also reduces heat loss, allowing for more efficient energy utilization. Secondly, surrounding heating can control the temperature around 1000K, effectively avoiding underground coal melting caused by excessively high flame temperatures. This temperature control is crucial for ensuring smooth coal seam reactions, as molten coal can not only damage the well wall structure but may also hinder the progress of internal chemical reactions within the coal seam.

5.2 Influence of Diverter Chamber Eccentric Angle on Combustion Flow Field

During the initial ignition stage of surrounding ignition heaters, oxygen supply relies solely on the oxygen within the gas mixing chamber, while the central oxygen pipeline temporarily does not supply oxygen. With constant mass flow rates (q) of acetylene and oxygen, as well as constant oxygen concentration (n), the eccentric angle of the diverter tube is adjusted to 0° , 10° , 20° , 30° , and 40° . Simulations of the underground combustion flow field are conducted under these five operating conditions. Changes in the eccentric angle of the diverter tube affect the length (L) of the high-temperature zone on the well wall. Specific data is presented in the following table:

Table 3. Heating Length Data of Combustion Flow Fields at Different Eccentric Angles

	$q_{C_2H_2}$ (g/s)	q_{O_2} (g/s)	L(m)	L_e (m)	T_e (K)
$\Theta=0^\circ$	1	1	0.665	0.331	1640
$\Theta=10^\circ$	1	1	0.67	0.282	1680
$\Theta=20^\circ$	1	1	0.65	0.257	1710
$\Theta=30^\circ$	1	1	0.49	0.097	2880
$\Theta=40^\circ$	1	1	0.375	0.095	2890

By analyzing the data in the table, it can be seen that, in terms of the efficient heating length of the well wall, there is a trend of first increasing and then decreasing as the eccentric angle increases. The maximum value of 0.67m is obtained at $\theta = 0^\circ$, while the minimum value of 0.375m, which is about 44% shorter than the maximum, is obtained at $\theta = 40^\circ$. The position of the highest well wall temperature tends to be towards the front, and the highest well wall temperature gradually increases, while the lowest well wall temperature is about 43% lower than the highest temperature.

The temperature contour maps of well wall heating at different eccentric angles are shown in Figure 8. The adjustment of the eccentric angle of the diverter chamber affects the fluid dynamics of the oxygen-acetylene mixture, which directly reflects in the flame shape and heat distribution. By carefully analyzing the combustion contour maps, it can be observed that when the eccentric angle is 0° , the flame exhibits a relatively symmetrical and uniform distribution. When the eccentric angle is slightly adjusted to 10° , although there are slight changes in the flame shape, it still maintains similar overall characteristics. However, it is worth noting that the heat transfer within the combustion chamber is more profound at this time, indicating that the penetration of heat within the channel has been optimized. As the eccentric angle further increases to 20° , the flame begins to shorten significantly, which means that the concentration of heat distribution increases but the overall coverage decreases. When the eccentric angle reaches 30° , the flame shape undergoes a fundamental change, no longer maintaining a single converging state but splitting into two independent flames that directly heat the well wall. As the eccentric angle continues to increase, this trend of flame separation becomes more pronounced, further affecting the distribution and utilization efficiency of heat.

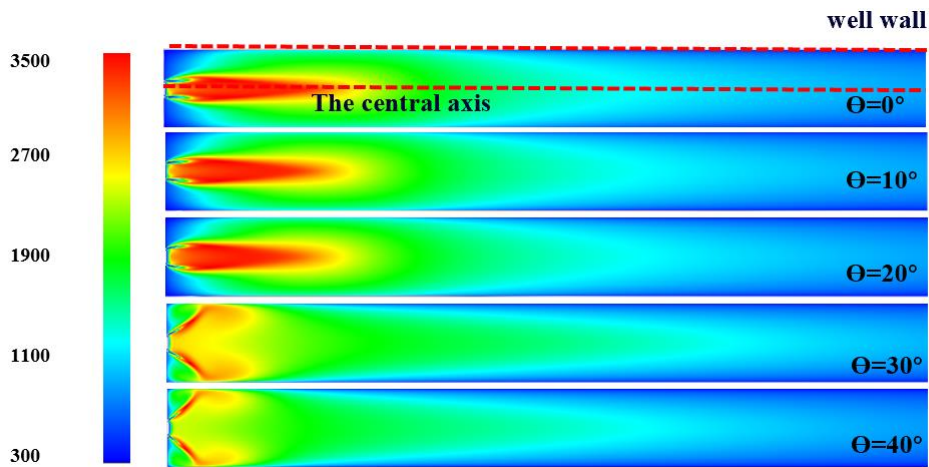


Figure 8. Temperature Contour Maps of Well Wall Heating at Different Eccentric Angles

By deeply analyzing the contour map data and specific experimental data, it can be found that changes in the eccentric angle have a complex impact on the well wall heating effect. The axial variation curves of well wall temperature at different eccentric angles are shown in Figure 9 (since the combustion flow field at a 40° eccentric angle is approximately equal to that at 30° , the axial variation curve of well wall temperature at 40° is not analyzed). On the one hand, the heating length of the well wall first increases and then gradually decreases as the eccentric angle increases, reflecting the dynamic balance between heat transfer and flame shape. On the other hand, the highest well wall temperature shows a continuous decreasing trend, while the position of the highest temperature continuously moves forward, and the position of the highest temperature on the central axis correspondingly moves backward. This indicates that the distribution of heat on the well wall becomes more uneven, with local high-temperature areas gradually shrinking and moving towards the front end. Additionally, the continuous shortening of the flame further confirms that as the eccentric angle increases, the concentration and local heating intensity of the flame increase, but the overall coverage area and uniformity decrease.

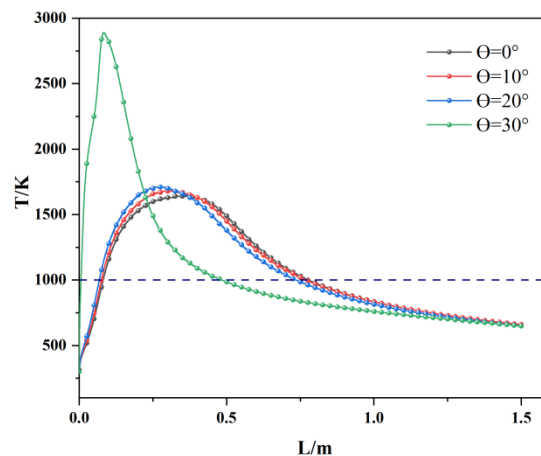


Figure 9. Axial Variation Curves of Well Wall Temperature at Different Eccentric Angles

In summary, by adjusting the eccentric angle of the diverter chamber, precise control of the flame shape and heat distribution can be achieved to optimize the well wall heating effect. In this study, the best well wall heating effect was observed at an eccentric angle of 10° , which ensures effective heat penetration while avoiding local overheating caused by excessive flame concentration.

6. Conclusion

In this paper, an innovative surrounding-type underground in-situ coal gasification igniter has been designed, and its internal flow channel has been simulated. To comprehensively evaluate the performance of this igniter, a comparative analysis of its combustion with that of a conventional igniter was conducted, and the variation laws of the combustion flow field under different eccentric angles were studied. By accurately measuring parameters such as the length of the high-temperature zone on the wellbore wall, the wellbore wall temperature, and the axial temperature, the working performance of the igniter was assessed, revealing the intrinsic laws governing the changes in the combustion flow field with eccentric angles. The main conclusions drawn are as follows:

- (1) The surrounding-type underground in-situ coal gasification igniter achieves pre-uniform mixing of fuel gas and oxygen by optimizing the gas flow path, demonstrating good internal pressure and gas flow velocity performance under standard operating conditions.
- (2) Compared to central-type surrounding-type underground in-situ coal gasification igniters, the flame of the proposed igniter exhibits axial expansion, with a more uniform heat distribution. It achieves better wellbore wall heating and superior flame penetration.
- (3) Increasing the eccentric angle causes the flame ejected from the igniter to primarily exhibit radial expansion. By adjusting the eccentric angle of the flow diverter, precise control over the flame shape and heat distribution can be achieved. An eccentric angle of 10° exhibits the optimal wellbore wall heating effect.

Funding Projects

Sub-project of the National Key Research and Development Program of China (Grant No. 2022YFC3005903–2);

General Program of the National Natural Science Foundation of China (Grant No. 42172345);

Graduate Innovation Fund Project of Jilin University (Grant No. 2024CX103).

References

- Adjei, S. T., Yindi, Z., Mengting, S., et al. (2023). Current status and technology development in implementing low carbon emission energy on underground coal gasification (UCG). *Frontiers in Energy Research*.
- Chandelle, V., Jacquemin, C., L  olle, R., et al. (1993). Underground coal gasification on the Thulin site: results of analysis from post-burn drillings. *Fuel*, 72(7), 949-963.

- [https://doi.org/10.1016/0016-2361\(93\)90292-A](https://doi.org/10.1016/0016-2361(93)90292-A)
- Hill, R. W., & Thorsness, C. B. (1982). *Summary report on large-block experiments in underground coal gasification, Tono Basin, Washington*. Volume 1. Experimental description and data analysis[R]. United States: Lawrence Livermore National Lab.
- Ma Xiaobo. (2014). Analysis of Mining Technology and Innovative Methods in Coal Mining. *Energy and Conservation*, 2014(08), 173-174.
- Mao, F. (2016). Underground coal gasification (UCG), A new trend of supply-side economics of fossil fuels. *Natural Gas Industry B*, 3(4), 312-322. <https://doi.org/10.1016/j.ngib.2016.12.007>
- Ranade, V., Mahajani, S., & Samdani, G. (2019). Computational modeling of underground coal gasification. *Computational Modeling of Underground Coal Gasification*. <https://doi.org/10.1201/9781315107967>
- Siemens C W. (1868). XXXIII. — On the regenerative gas furnace as applied to the manufacture of cast steel. *Journal of the Chemical Society*, 21(0), 279-310. <https://doi.org/10.1039/JS8682100279>
- Stefan, Z., Erika, S., Andrea, S., et al. (2021). The Usage of UCG Technology as Alternative to Reach Low-Carbon Energy. *Energies*, 14(13), 3718-3718. <https://doi.org/10.3390/en14133718>
- Yang Fu, Duan Zhonghui, Ma Dongmin, et al. (2020). Progress of Underground Coal Gasification Technology. *Science & Technology Review*, 38(20), 71-85.
- Zou Caineng, Chen Yanpeng, Kong Lingfeng, et al. (2019). Underground Coal Gasification and Its Strategic Significance for China's Natural Gas Development. *Petroleum Exploration and Development*, 46(02), 195-204. [https://doi.org/10.1016/S1876-3804\(19\)60002-9](https://doi.org/10.1016/S1876-3804(19)60002-9)